

Unveiling the distinctive geochemical signature of fine ware through Sr-Nd-Pb isotopes: A site-specific perspective from the site of Cales (South Italy)

Maria Verde¹  | Alberto De Bonis^{2,3}  | Massimo D'Antonio² 
 Virginie Renson⁴  | Stephen Czujko^{4,5}  | Antonella Tomeo⁶ | Vincenzo Morra² 

¹Dipartimento di Architettura, Università degli Studi di Napoli Federico II, Naples, Italy

²Dipartimento di Scienze della Terra, dell'Ambiente e delle Risorse, Università degli Studi di Napoli Federico II, Naples, Italy

³CRACS, Center for Research on Archaeometry and Conservation Science, Naples, Italy

⁴Research Reactor Center, University of Missouri, Columbia, Missouri, USA

⁵Classics, Archaeology, and Religious Studies Department, University of Missouri, Columbia, Missouri, USA

⁶Soprintendenza Archeologia Belle arti e Paesaggio per le Province di Caserta e Benevento, Caserta, Italy

Correspondence

Maria Verde, Dipartimento di Architettura, Università degli Studi di Napoli Federico II, Naples, Italy.

Email: maria.verde@unina.it

Alberto De Bonis, Dipartimento di Scienze della Terra, dell'Ambiente e delle Risorse, Università degli Studi di Napoli Federico II, Naples, Italy.

Email: alberto.debonis@unina.it

Scientific editing by Sarah Sherwood.

Funding information

National Science Foundation,
 Grant/Award Numbers: #2208558, #0922374

Abstract

This study explores the use of three isotopic systematics—Sr, Nd, and Pb—combined together for the first time to trace the origins of ancient pottery. This approach strengthens our ability to relate raw materials to the final products. The materials selected for the analysis are from a well-documented data set, previously subjected to a thorough mineralogical–petrographic and chemical characterization. Seventeen ceramic specimens represented by black-glazed pottery, Terra sigillata, and fine common ware as well as production indicators such as black-glazed pottery wasters and spacers were examined via isotope analyses. These samples were discovered in the archaeological site of Cales, presently Calvi Risorta, in South Italy. CaO-rich clay raw materials from the area of interest were also analyzed as comparative references for the investigated ceramics. The comparison of the archaeometric data of the ceramic samples with the clay raw materials showed an affinity between the ceramics studied and local clay raw materials belonging to Mio-Pliocene marine sediments from the Campania Apennine Mountain area. This affinity was more accurately defined through the Sr, Nd, and Pb isotopes, which show coinciding signatures among ceramic samples, production indicators, and raw materials. The method yields promising outcomes that reinforce prior experimental investigations and amplify its reliability. The multi-isotopic methodology highlights the significance of combining geochemical data to pinpoint the origins of raw materials used for ancient ceramic production.

KEY WORDS

binary mixing, fine ware, isotopes, local production, provenance

1 | INTRODUCTION

The mineralogical–petrographic approach has become an indispensable source of assistance in the study of archaeological ceramics. In provenance studies, the identification of the geological resources used for the manufacture of ancient ceramics remains challenging. Mineralogical–petrographic (e.g., polarized light microscopy, and scanning electron microscopy-energy-dispersive spectroscopy) and chemical (e.g., X-ray fluorescence [XRF], inductively coupled plasma–mass spectrometry [ICP-MS], and neutron activation analysis) techniques are applied to compare ceramics and raw materials (clays and temper), production indicators (e.g., kiln wastes, *instrumenta*, unfired pottery), and reference groups of target pottery production (Maggetti, 2001). However, the results obtained by these methods are not always conclusive, especially when fine ceramics are involved, as the a-plastic component is barely recognizable via polarized light microscopy. In this case, the chemical approach is well-suited, although still susceptible to biases due to possible chemical variations caused by raw material processing, such as levigation, or post-firing and secondary processes (De Bonis et al., 2013, 2018; Li et al., 2005, and references therein).

Recently, an encouraging contribution was provided by radiogenic isotopes analysis, which is gaining ground as a complementary method for sourcing ancient ceramics. Radiogenic isotopes have been considered in the geosciences as valuable tools for the geochemical characterization and origin identification of volcanic rocks and sedimentary clays (e.g., Faure & Mensing, 2005, and references therein). In the present study, the isotopic ratios of strontium (Sr), neodymium (Nd), and lead (Pb) were selected for specific reasons. These elements are commonly present in the minerals of a variety of rock types, including pyroclastic and sedimentary rocks, varying in concentration much more than major elements (e.g., Ca) do, thus being more sensitive to natural processes (Rollinson & Pease, 2021, and references therein). Furthermore, their isotopic compositions reflect the origin and geological history of the host rock, as demonstrated by a wealth of studies conducted in the past decades (Faure & Mensing, 2005, and references therein).

The use of radiogenic isotopes in ceramic provenance study has been explored in various cases, using either a single isotopic tracer (e.g., Carter et al., 2011; Li et al., 2005; Maritan et al., 2023; Renson, Jacobs, et al., 2013; Renson, Martínez-Cortizas, et al., 2013; Renson et al. 2016) or combining two isotopic systematics (e.g., De Bonis et al., 2018; Guarino et al., 2021; Kibaroglu et al., 2019; Li et al., 2006; Makarona et al., 2016; Renson et al., 2011). An important step ahead in this field was provided by De Bonis and co-authors in 2018, by an experimental study on ceramic replicas made with well-selected clays and different proportions of temper, which attested to the possibility to fingerprint the pottery combining Sr and Nd isotopic systematics in relation to the raw materials used.

The present study further explores the efficacy of the method by combining for the first time the three isotopic systematics—Sr, Nd, and Pb—for the analysis of pottery and raw materials. A group of samples from a well-constrained reference group of fine pottery

attested in Cales was selected. That town, corresponding to the modern Calvi Risorta (Caserta municipality, Campania, south Italy), was a Roman colony that became a thriving center of production and distribution of fine pottery classes. The investigated objects belong to an important production that took place in Cales during a well-identified period (3rd century B.C.E.–1st century B.C.E.) and primarily include production indicators, such as kiln wastes of black-glazed pottery, as well as selected specimens of Terra sigillata, fine common ware, and *instrumenta*.

The archaeological constraints of this ceramic production, along with site-specific and homogeneous compositional features revealed from the characterization made via conventional archaeometric analyses carried out by Verde et al. (2023), constitute an excellent case study to evaluate the efficacy of the approach proposed here. This allowed us to take a step forward after the encouraging results obtained via the Sr–Nd isotopic systematics, also by adding Pb systematics successfully applied in other studies, to provide more robust insights into pottery provenance and the complex processes involved in raw material sourcing and processing. This research demonstrates how valuable the multi-isotope approach is for provenance studies.

2 | THE SELECTED MATERIALS

2.1 | The pottery

The samples selected for the isotopic analyses come from a broader set of 79 samples of fine pottery belonging to the archaeological site of Cales that were characterized by a multi-analytical approach (Verde et al., 2023). The outcomes of those analyses highlighted that the studied materials hold significant value as they represent a reference group from the Cales site. This reference group includes various ceramic classes that were produced during a well-defined period spanning from the 3rd century B.C.E. to the 1st century B.C.E. The group included 57 specimens of black-glazed pottery (Figure 1a; Table 1), three samples of Terra sigillata pottery (Figure 1b; Table 1), nine samples of fine common ware (illustrated in Figure 1c and outlined in Table 1), and 10 objects associated with the production process. These production-related items serve as indicators and are represented by spacers and discarded fragments of fused black-glazed pottery (Figure 1d; Table 1). In archaeological terms, these objects are identified as *paterae*, *pissidi*, and cups, all characterized by their distinctive black surface coating.

Of particular interest are certain specimens categorized as black-glazed forms but showing a surface that transitions from black to red. This peculiarity potentially signifies errors in keeping the oxidizing conditions steady during the firing process and might represent early attempts at a technological advancement in terms of the firing atmosphere. Specifically, these shifts in appearance could indicate a transition from the production of black-glazed pottery to the manufacturing of red-slipped Terra sigillata pottery (as discussed by Soricelli, 2004).

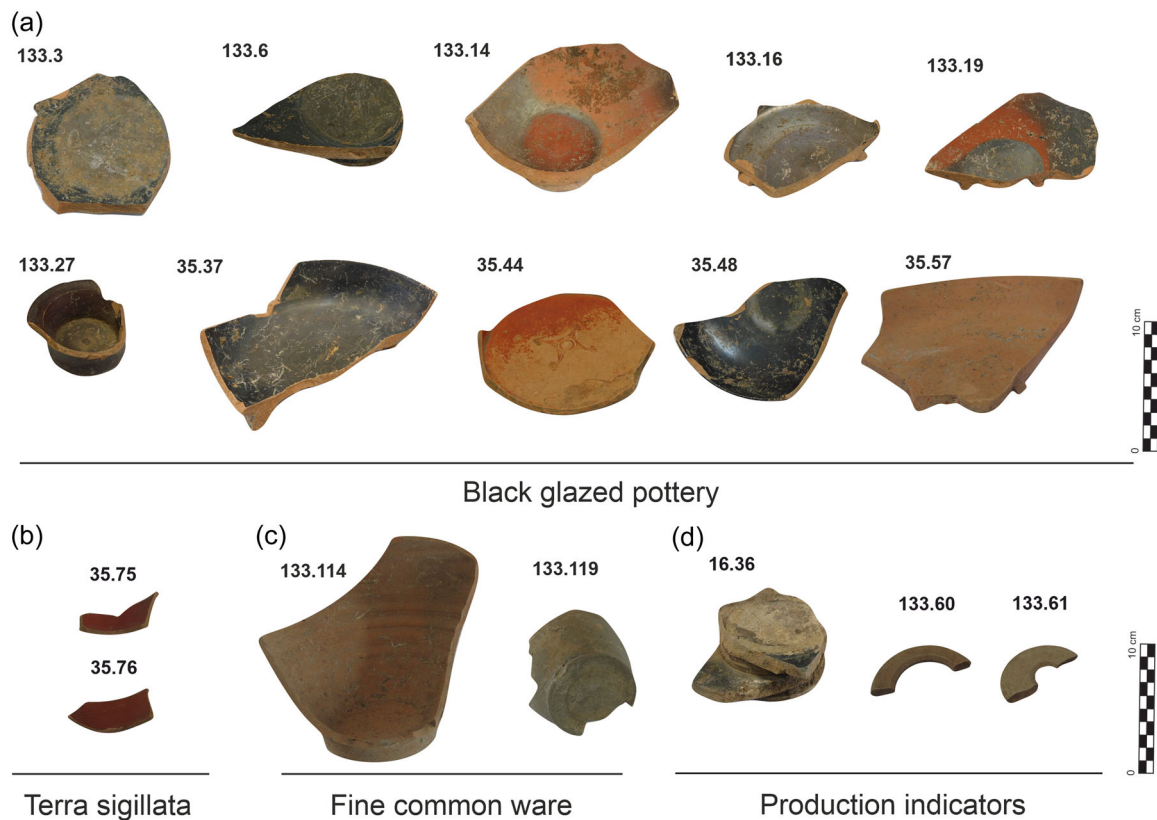


FIGURE 1 Selected samples of black-glazed pottery (a); Terra sigillata (b); fine common ware (c); production indicators; and (d) object of this study.

For the purposes of the present work, 17 representative specimens (Figure 1a-d) from the different ceramic classes were selected based on their petrographic characteristics, mineralogical assemblage, and chemical features (Verde et al., 2023; Table 1). The petrographic observation demonstrated a compositional homogeneity (Figure 2; Table 1). Almost all samples are fine-grained and characterized by an optically inactive and compact matrix; in some cases, diffuse birefringence is visible in the matrix due to recarbonated micro-crystalline calcite (Fabbri et al., 2014). The inclusions represent between 10% and 15% by volume and their size is generally lower than 200 μm . They are mostly composed of feldspar, quartz, mica, calcite, and rare lithic fragments of both volcanic (evident fragments of trachyte) and sedimentary nature (carbonate fragments), along with microfossils represented by planktonic foraminifers (Figure 2).

Additional information about the mineralogical assemblage comes from the XRPD (X-ray powder diffraction analysis) that revealed the presence of neoformed Ca silicates represented by gehlenite and pyroxene, indicating an EFT (Equivalent Firing Temperature) that generally ranges from 850°C to 1050°C, whereas just a few samples are characterized by an EFT from 750°C to 800°C (Table 1). The bulk chemistry shows that all the samples, including the production indicators, have a Ca-rich character and an extreme compositional homogeneity for both major oxides and trace elements.

These mineralogical and chemical aspects and their relationship with the composition of the raw materials used have been studied here

in more detail through isotopic analyses. Our focus was on highlighting the significance of the isotopic approach, shedding light on its role in pinpointing the origin of the pottery and on the ceramics' production processes, as well as its geological underpinnings.

2.2 | The raw materials

To identify the local products, all pottery was compared with clay raw materials coming from the surrounding area of Cales, likely used for the ceramic production (data from De Bonis et al., 2013). The geological frame of the surrounding area (Figure 3) is characterized by the Roccamonfina volcano to the north, composed of the oldest exposed post-orogenic volcanic rocks of Campania region (630–50 ka; Conticelli et al., 2009, and references therein; De Rita & Giordano, 1996). Mesozoic carbonate rocks (Latium–Campania–Molise carbonate platform; Bonardi et al., 2009) of the Trebulani Mountains crop out to the east. Immediately west of the town of Calvi Risorta, there are large clay deposits belonging to the foredeep succession of the Pietraroja Formation (Middle–Upper Tortonian), characterized by fine bedded argillitic marls and sandstones (Vitale & Ciarcia, 2018). The archaeological area of Cales is located on pyroclastic flow deposits from the best-known highest energy explosive eruption of Campi Flegrei, the Campanian Ignimbrite (ca. 40 ka, Giacco et al., 2017), and, subordinately, by the incoherent facies of the Neapolitan Yellow Tuff (ca. 15 ka,

TABLE 1 Summary of the main archaeological and compositional features of the selected samples from Verde et al. (2023).

| Sample ID | Class | Chronology | Form | Inclusions | Mineralogical assemblage | Equivalent firing temperatures (°C) |
|-----------|--------|--------------------------------|------------------|---|---------------------------------------|-------------------------------------|
| 133.3 | BG | Undated | Patera | Qz, Fsp, Cal, Mca, Volc./Sed. Lithics + fossils | Qz, Cal, Fsp, Px*, Gh* | 900–1000 |
| 133.6 | BG | Undated | Patera | Qz, Fsp, Cal, Mca, Volc./Sed. Lithics + fossils | Qz, Fsp, Px, Cal, Hem*, Gh* | 900–1000 |
| 133.14 | BG | Undated | Patera | Qz, Fsp, Cal, Mca, Volc./Sed. Lithics + fossils | Qz, Fsp, Cal, Hem*, Gh* | 900–1000 |
| 133.16 | BG | 2nd–1st cent. BCE | Cup base | Qz, Fsp, Cal, Mca, Volc./Sed. Lithics + fossils | Qz, Fsp, Px, Cal, Hem*, Gh* | 900–1000 |
| 133.19 | BG | Undated | Patera | Qz, Fsp, Cal, Mca, Volc./Sed. Lithics + fossils | Qz, Fsp, Cal, Hem*, Gh*, Mca/Ilt | 900–1000 |
| 133.27 | BG | Second half 2nd–1st cent. BCE | Pyxis | Qz, Fsp, Cal, Mca, Volc./Sed. Lithics + fossils | Qz, Fsp, Px*, Cal, Gh* | 900–1000 |
| 35.37 | BG | End 2nd–begin 1st cent. BCE | Cup | Qz, Fsp, Cal, Mca, Volc./Sed. Lithics + fossils | Qz, Fsp, Cal, Gh*, Mca/Ilt | 850–900 |
| 35.44 | BG | 2nd–1st cent. BCE | Patera/cup | Qz, Fsp, Cal, Mca, Volc./Sed. Lithics + fossils | Qz, Mca/Ilt, Fsp, Gh* | 750–850 |
| 35.48 | BG | 2nd cent. BCE | Cup | Qz, Fsp, Cal, Mca, Volc./Sed. Lithics + fossils | Qz, Fsp, Px*, Gh*, Mca/Ilt | 850–900 |
| 35.57 | BG | 2nd–1st cent. BCE | Cup | Qz, Fsp, Cal, Mca, Volc./Sed. Lithics + fossils | Qz, Fsp, Cal, Px*, Hem*, Gh*, Mca/Ilt | 850–900 |
| 35.75 | TS | End 1st cent. BCE/begin 1st CE | Cup | Qz, Fsp, Cal, Mca, Volc. Lithics | Qz, Cal, Mca/Ilt, Px*, Hem*, Gh* | 750–850 |
| 37.76 | TS | End 1st cent. BCE/begin 1st CE | Cup | Qz, Fsp, Cal, Mca, Volc. Lithics | Qz, Cal, Mca/Ilt, Px*, Hem*, Gh* | 750–850 |
| 133.114 | FCW | Undated | Base closed form | Qz, Fsp, Cal, Mca, Volc. Lithics | Qz, fsp, Cal, Gh*, Mca/Ilt, Hem* | 850–900 |
| 133.119 | FCW | Undated | Base closed form | Qz, Fsp, Cal, Mca, Volc. Lithics | Qz, Fsp, Px*, Gh* | 950–1050 |
| 16.36 | BG-W | Undated | Cup basis | Qz, Fsp, Cal, Mca, Volc./Sed. Lithics + fossils | Qz, Fsp, Px*, Cal, Gh* | >1050 |
| 133.60 | Spacer | Undated | Ring spacer | Qz, Fsp, Cal, Mca, Volc./Sed. Lithics + fossils | Qz, Fsp, Px*, Cal, Gh* | 950–1050 |
| 133.61 | Spacer | Undated | Ring spacer | Qz, Fsp, Cal, Mca, Volc./Sed. Lithics + fossils | Qz, Fsp, Px*, Cal, Gh* | 950–1050 |

Note: * , neofomed mineralogical phase.

Abbreviations: BG, black-glazed pottery; BG-W, black-glazed pottery waster; Cal, calcite; FCW, fine common ware; Fsp, feldspar; Gh, gehlenite; Hem, hematite; Ilt, illite; Mca, mica; Px, pyroxene; Qz, quartz; TS, Terra sigillata.

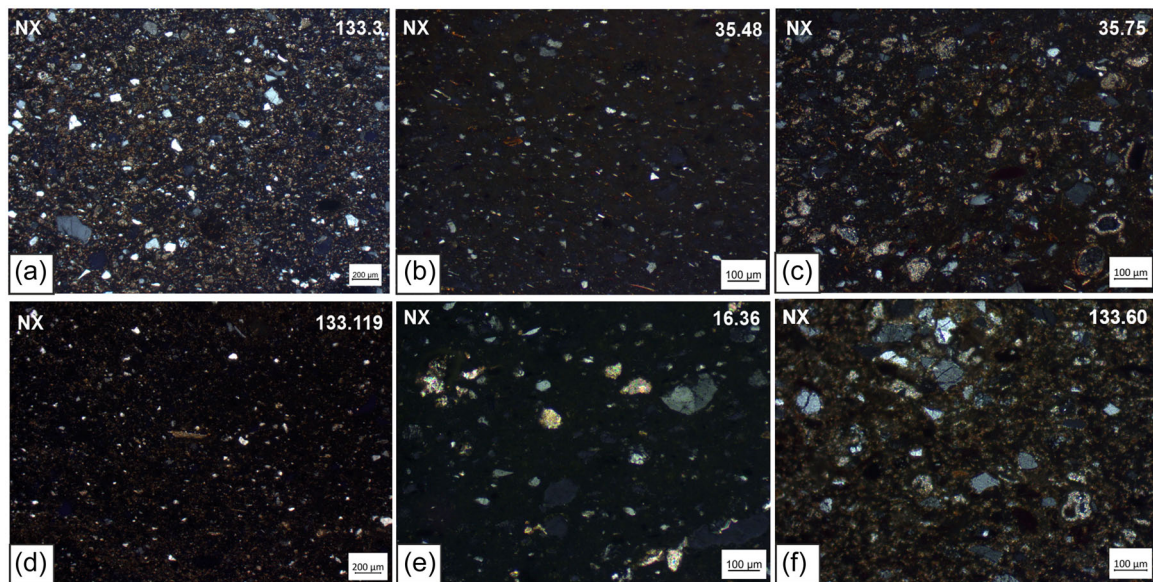


FIGURE 2 Thin-section images of black-glazed pottery (a, b); Terra sigillata (c); fine common ware (d) and production indicators (e, f). NX, crossed polars.

Galli et al., 2017), another well-known explosive eruption of the same volcanic field (see Orsi et al., 2022, for a review). A sample of volcanic trachyte sand (DUG1) ascribed to the Campanian Ignimbrite and currently used as a temper to produce traditional bricks (not far from the archaeological site of Cales) was analyzed as a representative material for local temper.

The clay raw materials selected for the isotopic comparison belong to marine deposits of Ca-rich clays from the Apennine sector ascribed to the Miocene Pietraroja Formation (Figure 3). Due to its optimal molding and sintering attitudes, this type of clay is suitable for making fine ceramics (De Bonis et al., 2013, 2014), as most of the pottery here investigated. Clay samples were collected in the quarries of Alvignano (ALV1-2) and Calvi Risorta (CVR1-2). The latter deposit is located just 3 km north-east of the archaeological site of Cales (Figure 3) and was used until recently for brick production (De Bonis et al., 2013; Guarino et al., 2011). The study by Verde et al. (2023) shows that these clays are fully compatible in terms of mineralogy and chemistry with the analyzed pottery.

3 | METHODS

To avoid any possible change in the lead composition due to the coating of black-glazed ware, the surface of pottery destined for the Pb isotopes analyses was mechanically cleaned before the powdering step with a microdrill equipped with silicon carbide bits, rinsed with DI water, and dried under heating lamps. That was not the case for Sr and Nd contents, for which no compositional changes were observed during trials with coated and uncoated specimens (Table S1). The choice to retain the coating during elemental chemistry analysis, as well as during subsequent Sr and Nd isotopic analysis, was suggested by

laboratory experiments. These experiments demonstrated that samples with and without the clay-based coating showed negligible variations in elemental chemistry (Table S1). Given the minimal impact of this coating on the elemental analytical results, it was concluded that removing the coating would have been unnecessary for isotopic analysis as well. In order to demonstrate this, the isotopes of Sr and Nd were reanalyzed on representative samples without coating, and the results of this experiment demonstrated negligible variability (Table S2).

3.1 | Elemental analysis of ceramic fragments

The concentrations of the chemical elements considered for the isotopic systematics were determined using different techniques on powders of the ceramic pastes. Chemical data of Sr were acquired via quantitative XRF carried out at the Dipartimento di Scienze della Terra, dell'Ambiente e delle Risorse (DiSTAR) laboratory, as described in Verde et al. (2023). For Pb and Nd, a fraction of the parent solution prepared for isotopic analyses was aliquoted for elemental analysis. The Pb and Nd concentrations were measured at the University of Missouri Research Reactor (MURR) by ICP-MS using a PerkinElmer Nexion 300X operated in KED mode. Solutions were prepared in 3% HNO₃ and internal standards of Sc, In, and Tl were added to the samples. The detection limits were below 0.0060 ppm Pb and 0.0095 ppm Nd.

3.2 | Pb isotope analysis

Clay samples were calcinated at 550°C for 4 h. Approximately 100 mg of powder was digested in closed Savillex® beakers (125°C, 48 h) in 2.5 mL of 24 N Trace Metal Grade HF and 0.5 mL of Optima

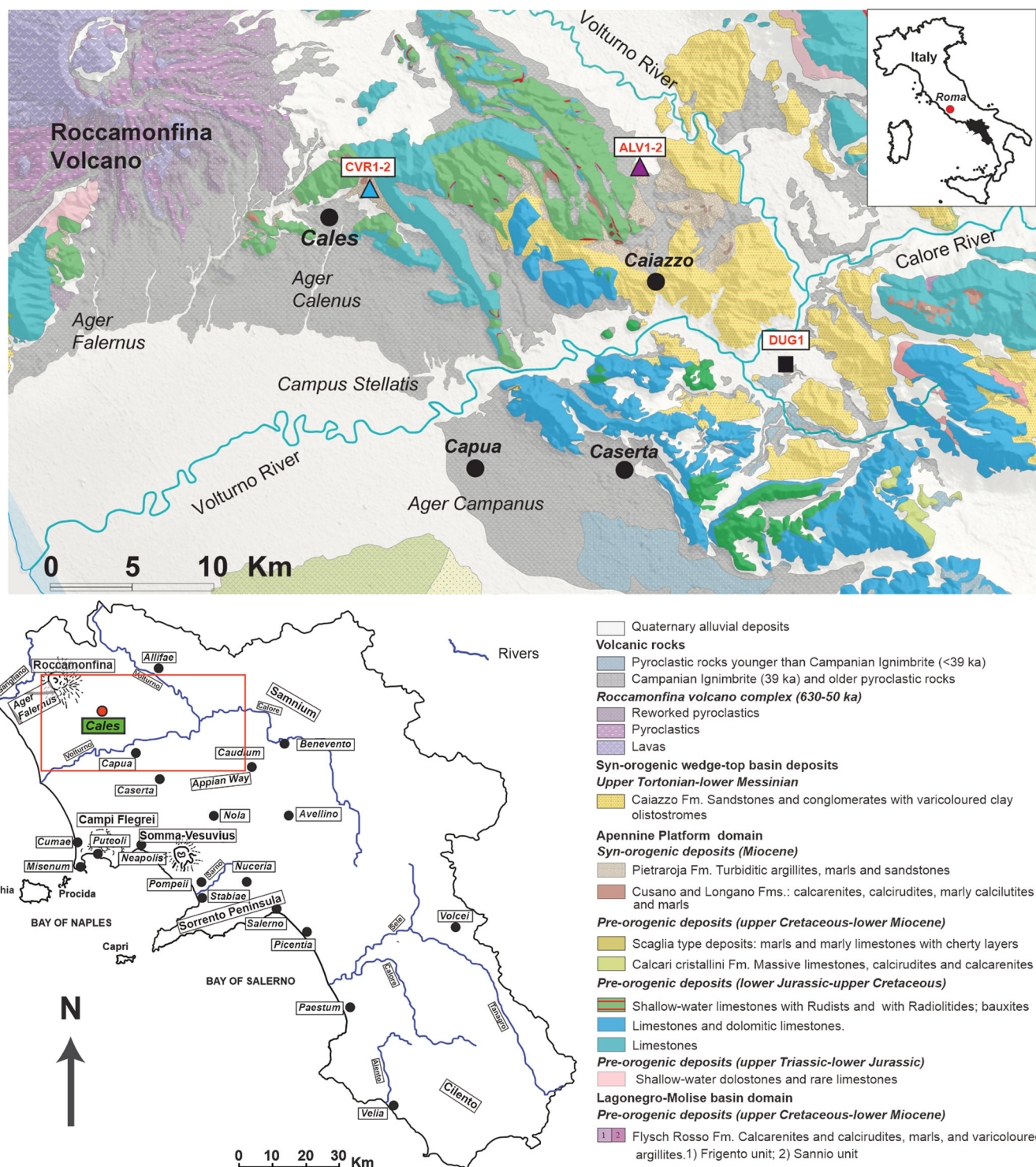


FIGURE 3 Geological sketch map of the northern Campania sector modified after Vitale and Ciarcia (2018).

Grade 14N HNO₃ and then evaporated at 90°C overnight. The dry residues were digested in 1.5 mL of Optima Grade 14N HNO₃, vials were closed and heated at 125°C for 48 h, and then evaporated at 90°C overnight. Lastly, the dry residues obtained were re-digested in 4 mL of 6N HCl at 125°C for 48 h and subsequently evaporated at 90°C overnight. The dry residues were finally dissolved in 2 mL

of 0.5M HBr. Lead extraction was undertaken via ion-exchange chromatography (BioRad AG1-X8 anion exchange resin) using a protocol adapted from Weis et al. (2006).

The analyses were conducted on a Nu Plasma II (Nu Instruments) Multi Collector–Inductively Coupled Plasma–Mass Spectrometer (MC-ICP-MS) in operation at the University of Missouri Research

Reactor (MURR). The instrument was optimized for ^{208}Pb maximum intensity (minimum signal of 150 mV at mass 204). The samples and standard were spiked using a TI solution to monitor and correct for mass fractionation. Sample solutions were prepared to measure Pb and TI concentrations similar to those of the NIST SRM981 international standard solution (approximately 200 ng g $^{-1}$ in Pb and 50 ng g $^{-1}$ in TI). The NIST SRM981 standard was measured several times at the beginning of each analytical session and after every two samples. Values were corrected for mass fractionation using the NIST value of 2.38714 for the $^{205}\text{TI}/^{203}\text{TI}$ natural ratio.

A correction for mercury isobaric interference at mass 204 was also applied using a 0.229883 value for the $^{204}\text{Hg}/^{202}\text{Hg}$ natural ratio. The mean values obtained for NIST SRM981 were 36.685 ± 0.012 (2 SD), 15.488 ± 0.002 (2 SD), and 16.936 ± 0.003 (2 SD) for $^{208}\text{Pb}/^{204}\text{Pb}$, $^{207}\text{Pb}/^{204}\text{Pb}$, and $^{206}\text{Pb}/^{204}\text{Pb}$ ratios, respectively.

The obtained data were corrected by standard-bracketing (Weis et al., 2006; White et al., 2000) using recommended values from Galer (1998). Two duplicates (i.e., entire procedure applied twice to the same sample), and two replicates (second analysis of the same solution) were measured to evaluate the reproducibility of measurements (Table 2).

3.3 | Sr-Nd isotope analysis

The Sr-Nd isotopic composition of representative fine ware and raw materials was determined using Thermal Ionization Mass Spectrometry (TIMS) techniques. Sample dissolution as well as Sr-Nd separation from the matrix were carried out within a Plexiglas laminar flow hood equipped with two HEPA filters located in an ISO 6 class clean room at DiSTAR (Naples, Italy). The samples were dissolved with Suprapur[®] grade HF-HNO₃-HCl acid mixtures (as for Pb isotopes). Sr and Nd were separated from the matrix using conventional cation-exchange chromatographic techniques on quartz columns filled with either AG[®] 50W-X8 (for Sr and Light Rare Earth Elements) or Ln Spec[®] (for Nd) resins and using diluted Suprapur[®] grade HCl as an eluant (Arienzo et al., 2013).

The Sr-Nd isotopic compositions of representative ceramic samples and raw materials (ALV1-2; CVR1, and DUG1) were determined at DiSTAR (Naples, Italy) using a Thermo Scientific Triton Plus[®] mass spectrometer. The instrument is equipped with one fixed and eight adjustable Faraday cups for simultaneous acquisition of several ion beams in static mode. The standard error with $N = 150$ was better than ± 0.000008 for both Sr and Nd measurements. During the period of analysis, replicate measurements of NIST SRM 987 (SrCO₃) and JNd-1 international reference standards were carried out to check for external reproducibility, 2σ (σ is the standard deviation of the standard results; Goldstein et al., 2003), obtaining the following mean values: $^{87}\text{Sr}/^{86}\text{Sr} = 0.710234 \pm 0.000013$ ($N = 48$) for NIST SRM 987 and $^{143}\text{Nd}/^{144}\text{Nd} = 0.512095 \pm 0.000006$ ($N = 31$) for JNd-1. The measured Sr and Nd isotope ratios were normalized to the recommended values of NIST-SRM 987 ($^{87}\text{Sr}/^{86}\text{Sr} = 0.710248 \pm 0.000012$ (σ); Zhang & Hu, 2020) and JNd-1 ($^{143}\text{Nd}/^{144}\text{Nd} = 0.512107 \pm 0.000012$ (σ); Zhang & Hu, 2020) standards, respectively.

$^{87}\text{Sr}/^{86}\text{Sr}$ and $^{143}\text{Nd}/^{144}\text{Nd}$ isotope ratios of CVR2 clay were determined at the Radiogenic Isotope Laboratory of the INGV-OV (Naples, Italy). Details on the analytical conditions are presented in De Bonis et al. (2018).

To determine the isotopic characteristics of the primary components (clays and temper) used in ceramic production and to define the origin of ancient pottery, various geological processes often lead to a combination of materials with distinct chemical and isotopic properties of elements like Sr, Nd, and Pb. In such instances, it is possible to compute the chemical and isotopic compositions of the resulting blends using simple models related to the theory of binary mixing (Langmuir et al., 1978) as detailed in De Bonis et al. (2018).

4 | RESULTS

4.1 | Elemental analysis

The obtained analytical results are presented in Tables 2 and 3, and in Figure S1. Most black-glazed pottery samples showed a very homogeneous Pb concentration (Figure S1a-c) ranging from 17 to 33 ppm (Table 2), apart from two samples, 133.119 and 35.44, which showed higher values of 48 and 96 ppm, respectively (Table 2). Specimens of the other ceramic classes are characterized by little variations in the elemental concentration of Pb that ranges from 20 to 21 ppm for Terra Sigillata, from 15 to 20 ppm for fine common ware, and from 12 to 26 ppm for the production indicator and spacers (Table 2). The Pb concentrations of raw materials (CVR1-2 and ALV1-2) are in line with the behavior of ceramics, virtually displaying the same concentrations (from 15 to 16 ppm), while the volcanic sand representing the temper (DUG1) shows a higher value (44 ppm).

The Sr elemental concentration (Figure S1d; Table 3) shows a narrow variability for all the investigated ceramics, which span from 313 ppm (Terra Sigillata sample 35.75) to 421 ppm (black-glazed sample 35.57); consistently, clay raw materials show very similar concentrations that range from 356 to 431 ppm (Table 2). In contrast, the volcanic temper shows a significantly higher value (526 ppm), a trend that is also consistent with the Nd concentration (Figure S1e; Table 3). Indeed, the temper shows the highest value (57 ppm), whereas the ceramics Nd ranges from 28 ppm (Terra Sigillata sample 35.76) to 34 ppm (black-glazed sample 35.48), mirroring the pattern seen in the clay raw materials that display similar concentrations (from 25 to 26 ppm).

4.2 | Pb isotope ratios

The results of the Pb isotopes analysis are reported in Table 2 and shown in Figure 4a,b. The Pb isotopic ratios of the black-glazed pottery are characterized by a narrow variability and range from 38.853 (sample 35.57) to 39.012 (sample 133.16) for $^{208}\text{Pb}/^{204}\text{Pb}$, from 15.668 (sample 35.57) to 15.692 (sample 133.16) for

TABLE 2 Elemental and isotope analyses of Pb of pottery and clay raw materials.

| Sample | Material | Class | Pb ppm | $^{208}\text{Pb}/^{204}\text{Pb}$ | 2 σe | $^{207}\text{Pb}/^{204}\text{Pb}$ | 2 σe | $^{206}\text{Pb}/^{204}\text{Pb}$ | 2 σe | $^{208}\text{Pb}/^{206}\text{Pb}$ | 2 σe | $^{207}\text{Pb}/^{206}\text{Pb}$ | 2 σe |
|---------|----------|--------|--------|-----------------------------------|--------------------|-----------------------------------|--------------------|-----------------------------------|--------------------|-----------------------------------|--------------------|-----------------------------------|--------------------|
| 133.3 | Pottery | BG | 21 | 38.999 | 0.002 | 15.690 | 0.001 | 18.844 | 0.001 | 2.06971 | 0.00003 | 0.83263 | 0.00001 |
| 133.6 | Pottery | BG | 19 | 38.994 | 0.001 | 15.694 | 0.001 | 18.833 | 0.001 | 2.07049 | 0.00002 | 0.83330 | 0.00001 |
| 133.14 | Pottery | BG | 33 | 38.960 | 0.002 | 15.688 | 0.000 | 18.800 | 0.001 | 2.07239 | 0.00002 | 0.83444 | 0.00001 |
| 133.16 | Pottery | BG | 19 | 39.012 | 0.002 | 15.692 | 0.001 | 18.841 | 0.001 | 2.07062 | 0.00003 | 0.83289 | 0.00001 |
| 133.19 | Pottery | BG | 48 | 38.987 | 0.002 | 15.683 | 0.001 | 18.777 | 0.001 | 2.07630 | 0.00004 | 0.83524 | 0.00001 |
| 133.27 | Pottery | BG | 27 | 38.972 | 0.002 | 15.688 | 0.001 | 18.803 | 0.001 | 2.07261 | 0.00003 | 0.83432 | 0.00001 |
| 35.37 | Pottery | BG | 17 | 38.989 | 0.002 | 15.687 | 0.001 | 18.856 | 0.001 | 2.06772 | 0.00003 | 0.83195 | 0.00001 |
| 35.44 | Pottery | BG | 96 | 38.984 | 0.002 | 15.685 | 0.001 | 18.744 | 0.001 | 2.07978 | 0.00003 | 0.83679 | 0.00001 |
| 35.48 | Pottery | BG | 24 | 38.945 | 0.002 | 15.680 | 0.001 | 18.856 | 0.001 | 2.06545 | 0.00003 | 0.83158 | 0.00001 |
| 35.57 | Pottery | BG | 22 | 38.853 | 0.002 | 15.668 | 0.001 | 18.738 | 0.001 | 2.07350 | 0.00003 | 0.83614 | 0.00001 |
| 35.75 | Pottery | TS | 21 | 38.928 | 0.002 | 15.682 | 0.001 | 18.818 | 0.001 | 2.06868 | 0.00003 | 0.83337 | 0.00001 |
| 35.76 | Pottery | TS | 20 | 38.909 | 0.002 | 15.682 | 0.001 | 18.809 | 0.001 | 2.06875 | 0.00002 | 0.83380 | 0.00001 |
| 133.114 | Pottery | FCW | 20 | 38.949 | 0.002 | 15.686 | 0.001 | 18.848 | 0.001 | 2.06649 | 0.00003 | 0.83222 | 0.00001 |
| 133.119 | Pottery | FCW | 15 | 39.038 | 0.003 | 15.703 | 0.001 | 18.818 | 0.001 | 2.07453 | 0.00003 | 0.83447 | 0.00001 |
| 1636 | Pottery | BG-W | 18 | 38.927 | 0.001 | 15.684 | 0.001 | 18.828 | 0.001 | 2.06750 | 0.00003 | 0.83301 | 0.00001 |
| 16.36* | Pottery | Spacer | 38.919 | 0.002 | 15.683 | 0.001 | 18.824 | 0.001 | 2.06755 | 0.00003 | 0.83314 | 0.00001 | |
| 16.36** | Pottery | Spacer | 38.919 | 0.003 | 15.683 | 0.001 | 18.824 | 0.001 | 2.06751 | 0.00003 | 0.83313 | 0.00001 | |
| 16.36** | Pottery | Spacer | 38.931 | 0.002 | 15.685 | 0.001 | 18.830 | 0.001 | 2.06754 | 0.00003 | 0.83302 | 0.00001 | |
| 133.60 | Pottery | Spacer | 12 | 38.969 | 0.002 | 15.686 | 0.001 | 18.850 | 0.001 | 2.06731 | 0.00003 | 0.83214 | 0.00001 |
| 133.61 | Pottery | Spacer | 26 | 38.965 | 0.002 | 15.684 | 0.001 | 18.805 | 0.001 | 2.07213 | 0.00004 | 0.83405 | 0.00001 |
| CVR1 | Clay | - | 16 | 38.943 | 0.003 | 15.687 | 0.001 | 18.831 | 0.001 | 2.06260 | 0.00004 | 0.83086 | 0.00001 |
| CVR1* | | | | 38.957 | 0.002 | 15.687 | 0.001 | 18.885 | 0.001 | 2.06287 | 0.00003 | 0.83067 | 0.00001 |
| CVR2 | Clay | - | 15 | 38.953 | 0.003 | 15.688 | 0.001 | 18.882 | 0.001 | 2.06294 | 0.00003 | 0.83082 | 0.00001 |
| ALV1 | Clay | - | 15 | 38.933 | 0.004 | 15.684 | 0.002 | 18.844 | 0.001 | 2.06607 | 0.00004 | 0.83231 | 0.00001 |
| ALV2 | Clay | - | 16 | 38.949 | 0.002 | 15.686 | 0.001 | 18.857 | 0.001 | 2.06551 | 0.00004 | 0.83187 | 0.00001 |
| DUG1 | Temper | - | 44 | 39.290 | 0.002 | 15.700 | 0.001 | 19.159 | 0.001 | 2.05062 | 0.00003 | 0.81940 | 0.00001 |

Note: Duplicate is denoted by *, while replicate is denoted by **.

Abbreviations: BG, black-glazed pottery; BG-W, black-glazed pottery waste; FCW, fine common ware; TS, Terra sigillata.

TABLE 3 Elemental and isotope analyses of Sr and Nd of pottery and clay raw materials.

| Sample | Material | Class | Sr ppm | Nd ppm | $^{87}\text{Sr}/^{86}\text{Sr}$ | 2se | $^{143}\text{Nd}/^{144}\text{Nd}$ | 2se |
|---------|----------|--------|--------|--------|---------------------------------|----------------|-----------------------------------|----------------|
| 133.3 | Pottery | BG | 364 | 33 | 0.710668 | ± 0.000006 | 0.512156 | ± 0.000005 |
| 133.6 | Pottery | BG | 360 | 30 | 0.710649 | ± 0.000006 | 0.512147 | ± 0.000005 |
| 133.14 | Pottery | BG | 337 | 30 | 0.710942 | ± 0.000007 | 0.512138 | ± 0.000004 |
| 133.16 | Pottery | BG | 360 | 31 | 0.710670 | ± 0.000006 | 0.512143 | ± 0.000004 |
| 133.19 | Pottery | BG | 342 | 30 | 0.710765 | ± 0.000006 | 0.512145 | ± 0.000005 |
| 133.27 | Pottery | BG | 333 | 31 | 0.710727 | ± 0.000007 | 0.512148 | ± 0.000005 |
| 35.37 | Pottery | BG | 345 | 31 | 0.710676 | ± 0.000007 | 0.512121 | ± 0.000005 |
| 35.44 | Pottery | BG | 355 | 33 | 0.710810 | ± 0.000007 | 0.512153 | ± 0.000005 |
| 35.48 | Pottery | BG | 357 | 34 | 0.710782 | ± 0.000006 | 0.512146 | ± 0.000005 |
| 35.57 | Pottery | BG | 421 | 32 | 0.710359 | ± 0.000006 | 0.512148 | ± 0.000005 |
| 35.75 | Pottery | TS | 313 | 32 | 0.710814 | ± 0.000007 | 0.512159 | ± 0.000005 |
| 35.76 | Pottery | TS | 339 | 28 | 0.710691 | ± 0.000007 | 0.512161 | ± 0.000005 |
| 133.114 | Pottery | FCW | 345 | 30 | 0.710874 | ± 0.000007 | 0.512155 | ± 0.000004 |
| 133.119 | Pottery | FCW | 394 | 30 | 0.710492 | ± 0.000006 | 0.512139 | ± 0.000005 |
| 16.36 | Pottery | BG-W | 339 | 32 | 0.710714 | ± 0.000006 | 0.512133 | ± 0.000006 |
| 133.60 | Pottery | Spacer | 366 | 30 | 0.710634 | ± 0.000007 | 0.512142 | ± 0.000005 |
| 133.61 | Pottery | Spacer | 357 | 30 | 0.710676 | ± 0.000006 | 0.512142 | ± 0.000005 |
| CVR1 | Clay | - | 379 | 26 | 0.711110 | ± 0.000006 | 0.512130 | ± 0.000005 |
| CVR2 | Clay | - | 431 | 25 | 0.710540 | ± 0.000009 | 0.512142 | ± 0.000007 |
| ALV1 | Clay | - | 356 | 25 | 0.710650 | ± 0.000006 | 0.512141 | ± 0.000005 |
| ALV2 | Clay | - | 366 | 26 | 0.710703 | ± 0.000007 | 0.512130 | ± 0.000005 |
| DUG1 | Temper | - | 526 | 57 | 0.707272 | ± 0.000006 | 0.512487 | ± 0.000006 |

Abbreviations: BG, black-glazed pottery; BG-W, black-glazed pottery waste; FCW, fine common ware; TS, Terra sigillata.

$^{207}\text{Pb}/^{204}\text{Pb}$, and between 18.738 (sample 35.57) and 18.856 (sample 35.37) for $^{206}\text{Pb}/^{204}\text{Pb}$ ratios. The lead isotopic values of the Terra sigillata samples range from 38.909 (sample 35.76) to 38.928 (sample 35.75) for $^{208}\text{Pb}/^{204}\text{Pb}$, from 15.682 (sample 35.75) to 15.682 (sample 35.76) for $^{207}\text{Pb}/^{204}\text{Pb}$, and between 18.809 (sample 35.76) and 18.818 (sample 35.75) for $^{206}\text{Pb}/^{204}\text{Pb}$. These isotopic ratios are compatible with the black-glazed pottery described above. The Pb isotopic compositions of fine common ware range from 38.949 (sample 133.114) to 39.038 (sample 133.119) for $^{208}\text{Pb}/^{204}\text{Pb}$, between 15.686 (sample 133.114) and 15.703 (sample 133.119) for $^{207}\text{Pb}/^{204}\text{Pb}$, and from 18.818 (sample 133.119) to 18.848 (sample 133.114) for $^{206}\text{Pb}/^{204}\text{Pb}$. In detail, sample 133.119 shows a higher value of the $^{207}\text{Pb}/^{204}\text{Pb}$ ratio that differs from the values of the other fine ceramics (Figure 4a). The $^{208}\text{Pb}/^{204}\text{Pb}$, $^{207}\text{Pb}/^{204}\text{Pb}$, and $^{206}\text{Pb}/^{204}\text{Pb}$ ratios for the production indicators range from 38.927 (sample 16.36) to 38.969 (sample 133.60), from 15.684 (samples 16.36 and 133.61) to 15.686 (sample 133.60), and from 18.805 (sample 133.61) to 18.850 (sample 133.60), respectively.

The clays are characterized by a Pb isotopic composition that ranges from 38.933 (sample ALV1) to 38.953 (sample CVR2) for

$^{208}\text{Pb}/^{204}\text{Pb}$, from 15.684 (sample ALV1) to 15.688 (sample CVR2) for $^{207}\text{Pb}/^{204}\text{Pb}$, and between 18.844 (sample ALV1) and 18.882 (sample CVR2) for $^{206}\text{Pb}/^{204}\text{Pb}$ ratios. On the other hand, the $^{208}\text{Pb}/^{204}\text{Pb}$, $^{207}\text{Pb}/^{204}\text{Pb}$, and $^{206}\text{Pb}/^{204}\text{Pb}$ ratios for the temper are 39.290, 15.700, and 19.159, respectively.

4.3 | Sr and Nd isotope ratios

The results show that the black-glazed pottery has $^{87}\text{Sr}/^{86}\text{Sr}$ isotope ratios varying from 0.710359 (sample 35.57) to 0.710942 (sample 133.14) and $^{143}\text{Nd}/^{144}\text{Nd}$ ratios varying from 0.512121 (sample 35.37) to 0.512156 (sample 133.3), thus showing a narrow isotopic variability (Figure 5; Table 3).

The Terra sigillata samples are characterized by an $^{87}\text{Sr}/^{86}\text{Sr}$ isotope ratio between 0.710691 (sample 35.76) and 0.710814 (sample 35.75) and a $^{143}\text{Nd}/^{144}\text{Nd}$ isotope ratio between 0.512159 (sample 35.75) and 0.512161 (sample 35.76), which correspond to the isotopic ratios of Sr and Nd of the black-glazed pottery described above (Table 3; Figure 5).

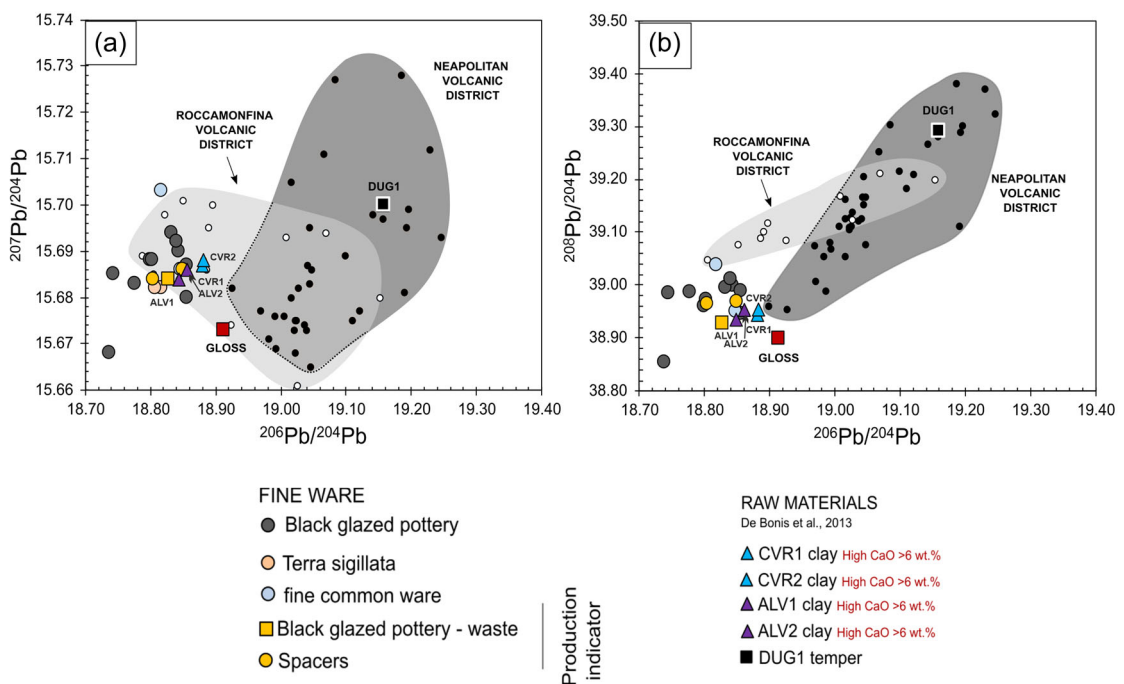


FIGURE 4 (a) $^{206}\text{Pb}/^{204}\text{Pb}$ vs $^{207}\text{Pb}/^{204}\text{Pb}$; (b) $^{206}\text{Pb}/^{204}\text{Pb}$ vs $^{208}\text{Pb}/^{204}\text{Pb}$ isotopic ratios measured on selected fine ware compared with some Ca-rich Campanian raw materials. The dark gray field represents the isotopic composition of Neapolitan volcanic products (Data from D'Antonio et al., 1996, 2007; Pappalardo et al., 2002). The light gray field represents the isotopic composition of the Roccamonfina volcano (Data from Conticelli et al., 2009).

The $^{87}\text{Sr}/^{86}\text{Sr}$ isotope ratio of the fine common ware varies from 0.710492 (sample 133.119) to 0.710874 (sample 133.114), while the $^{143}\text{Nd}/^{144}\text{Nd}$ isotope ratio ranges from 0.512139 (sample 133.119) to 0.512155 (sample 133.114). The isotopic ratios of Sr and Nd also appear to be consistent with the ceramic classes previously described (Table 3; Figure 5).

The isotopic signature of spacers shows an $^{87}\text{Sr}/^{86}\text{Sr}$ isotope ratio varying from 0.710634 (sample 133.60) to 0.710676 (sample 133.61) and the same $^{143}\text{Nd}/^{144}\text{Nd}$ isotope ratio (0.512142), which perfectly matches with the other ceramic classes.

Lastly, the production indicator represented by a stack of welded plates of black-glazed pottery shows an $^{87}\text{Sr}/^{86}\text{Sr}$ isotope ratio of 0.710714 and a $^{143}\text{Nd}/^{144}\text{Nd}$ isotope ratio of 0.512133, proving to be extremely compatible with the black-glazed pottery (Table 3; Figure 5).

The clay samples (Table 3; Figure 5) are characterized by an $^{87}\text{Sr}/^{86}\text{Sr}$ isotope ratio that varies from 0.710540 (sample CVR2) to 0.711110 (sample CVR1) and a $^{143}\text{Nd}/^{144}\text{Nd}$ isotope ratio that ranges from 0.512130 (samples CVR1 and ALV1) to 0.512142 (sample CVR2), whereas the selected temper (DUG1) shows an $^{87}\text{Sr}/^{86}\text{Sr}$ isotope ratio of 0.707272 and a $^{143}\text{Nd}/^{144}\text{Nd}$ isotope ratio of 0.512479.

5 | DISCUSSION

The studies conducted at the DiSTAR's labs (Naples, Italy) tested both experimentally (De Bonis et al., 2018) and on archaeological pottery (Guarino et al., 2021) the validity of Sr and Nd isotopes for ceramics

manufactured in the Greater Bay of Naples Region (Guarino et al., 2021), an area of southern Italy renowned worldwide for its rich and unique archaeological record including settlements, such as Pompeii, Herculaneum, Stabiae, Neapolis, Puteoli, and Cumae.

The effectiveness of Pb isotopes for determining different raw material sources has been demonstrated by Renson, Jacobs, et al. (2013a), and Renson, Martínez-Cortizas, et al. (2013b), comparing different geological materials with ceramic samples. Interesting results were also highlighted when manipulation processes used in ceramic technology were considered. In the case of Bronze Age ceramics (White Slip ware) from Cyprus studied by Renson, Martínez-Cortizas, et al. (2013), for which a local source of weathered gabbro was inferred as the raw material used, the value of the $^{207}\text{Pb}/^{204}\text{Pb}$ ratio remained unchanged after the levigation process carried out during clay processing.

In our study, the three isotopic systematics were applied on 17 ceramic samples representative of a well-defined reference group of the Calenian fine ware production and production indicators, the latter representing a robust marker to confirm the local provenance, further strengthening the reliability of the method. Indeed, the results of lead isotopes analysis leave no doubt about the compositional homogeneity of the ceramic classes of fine ware investigated and related production indicators represented by welded plates of black-glazed pottery along with spacers used inside the kiln. The latter are, by definition, untradeable items and are a very important term of comparison to assess with certainty the local manufacture of fine pottery. Furthermore, the investigated ceramics show a close

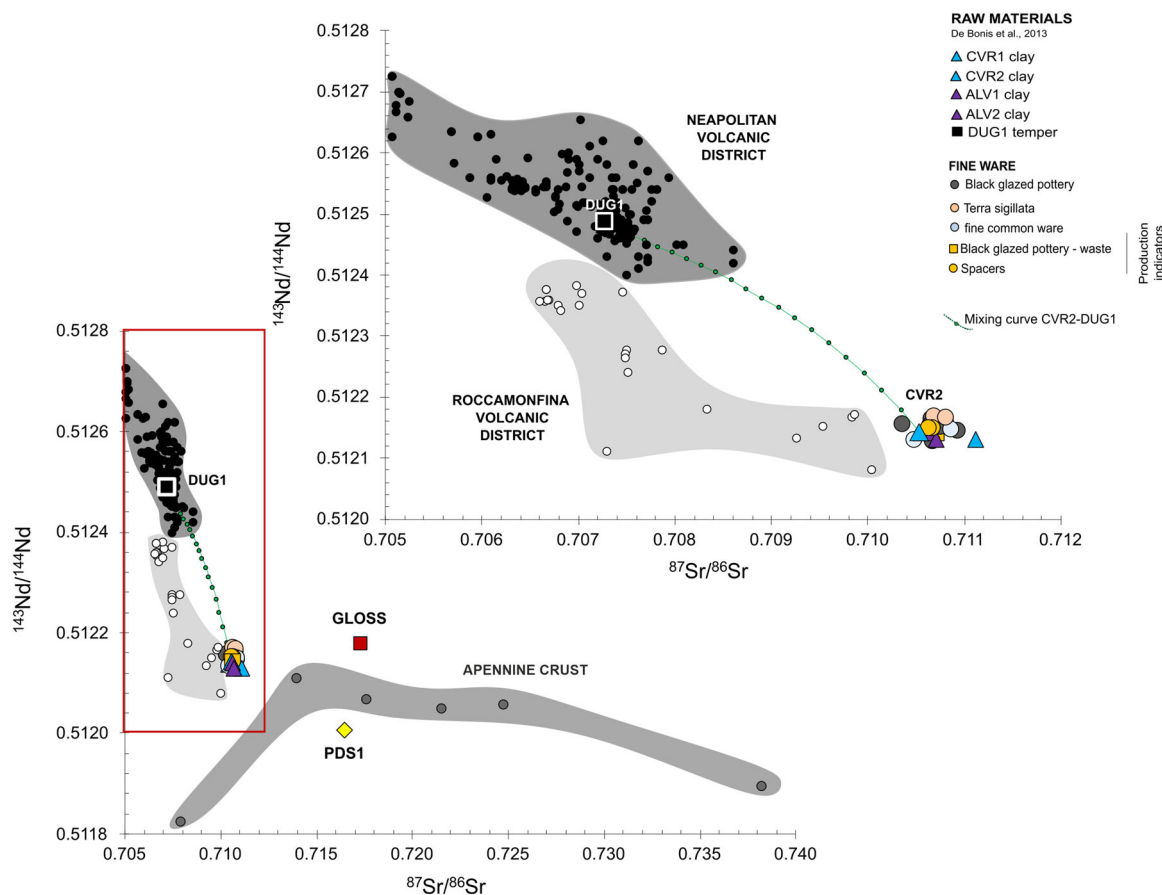


FIGURE 5 $^{87}\text{Sr}/^{86}\text{Sr}$ and $^{143}\text{Nd}/^{144}\text{Nd}$ isotopic ratios of raw materials and the fine ware selected for this study. The dark gray field represents the isotopic composition of Neapolitan volcanic products (Data from Brown et al., 2014; Carter et al., 1978; Conticelli et al., 2002, 2009; D'Antonio et al., 2007, 2013, 2016; De Astis et al., 2004; Di Renzo et al., 2007, 2011; Hawkesworth & Vollmer, 1979; Pabst et al., 2008; Paone, 2006; Tonarini et al., 2009). The light gray field represents the isotopic composition of the Roccamonfina volcano (Data from Carter et al., 1978; Conticelli et al., 2002, 2009). The moderate gray field is represented by the Apennine crust (Conticelli et al., 2002).

mineralogical and geochemical affinity with the Mio-Pliocene basin sediments of the local Apennine chain sector (ALV1-2, CVR1-2), which include the local clay deposit represented by the two CVR samples. The latter were most likely used as a supply source to produce fine pottery in Cales. It is noteworthy that the examined samples show a remarkable homogeneity also in terms of elemental chemistry. Comparing the elemental concentrations with the Pb isotopic ratios of all samples (Figure S1; Tables 2 and 3), it is evident that the fine ceramic samples selected for this study show a strong association with the local clay raw material.

In order to broaden the comparison with raw materials, sediments from around the world were included and the Pb isotopic signature of the GLOSS (GLObal Subducted Sediment; Plank & Langmuir, 1998) was also plotted (Figure 4), because it is dominated by terrigenous material that includes marine clays. GLOSS shows a good affinity with the group of pottery and clays, likely because lead is mostly hosted in the silicate fraction (e.g., Faure & Mensing, 2005, and references therein).

The lead isotopic composition of the volcanic sand representative of a local temper (DUG1) instead differs from that of the group

including pottery and clays (Figure 4). Its composition is in line with the Pb isotope signature of products from the Neapolitan volcanic district (Figure 4; data from D'Antonio et al., 1996, 2007; Pappalardo et al., 2002) that, apart from a partial overlap, tend to differ from the signature of the volcanic rocks from the Northern Campania region that belong to the Roccamonfina volcano (data from Conticelli et al., 2009).

The Sr-Nd method was applied on the same set of representative ceramic samples and raw materials (Table 3), in order to build a complete Pb-Sr-Nd isotope data set. Following the outcomes from the experimental study by De Bonis et al. (2018) that clearly demonstrated the effect of the temper on the isotope ratio of a clay-temper mixture, a theoretical mixing curve (Figure 5) was constructed by using the local clay (CVR2) and the volcanic temper (DUG1) to represent the two end-members. The Sr-Nd isotope compositional fields of the products from the Neapolitan volcanic district and the Roccamonfina volcanic district were also reported for comparison (Figure 5; data from De Astis et al., 2004; Brown et al., 2014; Carter et al., 1978; Conticelli et al., 2002; Conticelli et al., 2009; D'Antonio et al., 2007, 2013, 2016; Hawkesworth &

Vollmer, 1979; Pabst et al., 2008; Paone, 2006; Di Renzo et al., 2007, 2011; Tonarini et al., 2009). As expected, based on the Pb isotope evidence, the Roccamontefina products are very distinct both from the temper, which is clearly associated with Neapolitan products (i.e., trachytic rocks from Campi Flegrei), and from the group including pottery and clays (Figure 5). The decision to include the data of the volcanic materials was made to verify a possible compositional change due to the presence of a small amount of fine-grained volcanic (trachyte) lithics found in the pottery (Verde et al., 2023). This aligns with the intended use of these ceramics, as they belong to the category of fine ceramics primarily utilized for decorative and votive purposes. As volcanic inclusions are not naturally contained in the marine sediments from the area of interest (CVR and ALV samples), the presence of volcanic inclusions could be due either to a reworking of the clay deposits or, more likely, a purposeful addition by potters as a component of the mixture. The latter occurrence could justify the use of a plasticity corrector to optimize a mass-scale production such as that from Cales (Pedroni, 2001; Verde et al., 2023).

The 17 ceramic samples under study, including black-glazed pottery, Terra sigillata, fine common ware, and production indicators, show virtually no variations and this is clear from the Sr-Nd isotopic mixing plot, where the negligible amount of volcanic temper does not affect the position of the pottery samples, which cluster around CVR and ALV clay raw materials (Figure 5). Given the very fine grain size of the clays in question, they behave as homogeneous materials, yielding homogeneous values of the 3 isotopic ratios, even though they are composed of different types of clay minerals and other phases that incorporate Sr, Nd, and Pb in different amounts, depending on the different affinity of Sr and Pb (replacing K and Ca) and Nd (replacing several major bivalent cations, especially in feldspar minerals; Faure & Mensing, 2005, and references therein).

The clays selected for this study have been the subject of an extensive program of survey and analysis carried out to identify the potential sources of raw materials for ancient ceramics in the Campania region of Italy (De Bonis et al., 2013). They were selected both for their proximity to the site of Cales and for their technological features, which are well suited to the manufacture of fine ceramics (De Bonis et al., 2013, 2014). Geologically speaking, they are Ca-rich clays belonging to Neogene synorogenic foredeep basin deposits from the Apennine chain (Vitale & Ciarcia, 2018) and show homogeneous Sr and Nd isotope ratios. Their typical isotopic fingerprint strictly depends on their common geological origin. Therefore, when different sediments such as the GLOSS (Figure 5), representative rocks from the Apennine crust (Conticelli et al., 2002), or older Campania clays (sample PDS1, $^{87}\text{Sr}/^{86}\text{Sr} = 0.716450$, $^{143}\text{Nd}/^{144}\text{Nd} = 0.512007$; see Guarino et al., 2021 for details) deposited in pre-orogenic deep basins are considered, a different Sr- and Nd-isotope signature is noticed.

Therefore, our attention must focus on the two clay deposits (ALV and CVR), which have the same isotopic fingerprint of the ceramics. These two clay deposits are the most volumetrically extensive in the investigated area, so they can be considered as potential sources of supply for ceramic production. The one in Calvi

Risorta (CVR) is located at ca. 3 km from the workshops of Cales, while the clay from Alvignano (ALV) is located at about 30 km. The latter source must be ruled out because it is available from a longer distance, so that it would not have made sense for the craftsmen to obtain a similar material, also in terms of processing features, but logically more unfavorable (see Arnold, 2006).

Furthermore, it should be considered that the presence of geological resources, such as high-quality clays, would have given rise to production centers in antiquity that gravitated around clay deposits. This is very likely the case of Cales, where high-quality clays, belonging to marine deposits of the Apennine chain, are particularly suited for the production of fine ware with no or limited pre-processing.

In summary, the isotopic method seems to have provided an improvement in discriminating differences and homogeneities among the investigated samples. The larger variability observed with the measurement of elemental Pb (Figure S1a-c) is significantly reduced once isotopic data are considered (Figure 4), which demonstrates the strong homogeneity of fine ceramics and the analyzed clays, lending support to the overall coherence of the data set of Verde et al. (2023). This is also true when elemental Sr concentration is compared to Sr isotopic composition (Figure S1a). Considering the volcanic sand representing the temper (DUG1), a far better discrimination from the other investigated samples is evidenced by the isotopic method (Figure S1).

The application of Pb, Sr, and Nd isotopic systematics used in this study highlighted the potential of radiogenic isotope analysis applied to determine the origin of ancient ceramics and search for possible sources of raw material used by the ancient craftsmen.

6 | CONCLUSIONS

The approach proposed here was applied to a well-constrained archaeological case involving a local reference group of fine pottery from Cales, which includes different ceramic classes of fine ware (black-glazed ware, Terra sigillata, fine common ware) and the related production indicators (wasters and spacers). By applying three isotopic systematics (Sr-Nd-Pb) for the first time for the investigation of pottery provenance, this study verified the reliability of the isotopic method to explore archaeological ceramics, especially when combined with in-depth mineralogical-petrographic characterization. This approach represents a valuable tool for investigating pottery provenance, pinpointing the sources of raw materials, and their possible processing before shaping.

In the case of Cales, the isotopic fingerprint of fine-grained ware is in line with the clay raw material used, given the negligible occurrence of a different material (i.e., volcanic temper) in the base clay. These results are significant for the evidence that they provided regarding the sources of raw material. Craftsmen at Cales used marine clays lying in the immediate environs of the town (3 km away from the production center) for a mass-scale production of fine pottery.

This research highlights the key role of isotopic systematics as a valid support to the analytical routine used for the archaeometric characterization of ceramics, which aims not only at identifying their provenance but also helping to reconstruct the potential recipes used by ancient craftsmen. Our next research objective will expand this methodology to a broader data set, including ceramics of different use and fabric. The goal will be a more in-depth study of coarse-grained ceramics, which could provide more information to determine the precise clay-temper ratio.

AUTHOR CONTRIBUTIONS

Maria Verde: Conceptualization; investigation; methodology; formal analysis; data curation; writing—original draft; writing—review and editing; visualization. **Alberto De Bonis:** Conceptualization; investigation; methodology; formal analysis; data curation; writing—review and editing; supervision; project administration; funding acquisition; validation. **Massimo D'Antonio:** Investigation; methodology; formal analysis; data curation; writing—review and editing; validation. **Virginie Renson:** Investigation; methodology; formal analysis; data curation; writing—review and editing; funding acquisition; validation. **Stephen Czujko:** Investigation; methodology; formal analysis; writing—review and editing. **Antonella Tomeo:** Conceptualization; investigation; resources; writing—review and editing. **Vincenzo Morra:** Conceptualization; investigation; writing—review and editing; supervision; project administration; funding acquisition; validation.

ACKNOWLEDGMENTS

The authors would like to thank Dr. Ilenia Arienzo for her support in the measurement of some Sr-Nd isotopes at the INGV-OV (Naples, Italy) and Jim Guthrie for ICP-MS data acquisition at MURR. This work was supported by grants from the DiSTAR (Alberto De Bonis, Vincenzo Morra and Massimo D'Antonio) of the University of Naples Federico II. The acquisition of the Nu Plasma II MC-ICP-MS at MURR was funded by the National Science Foundation grant #0922374. The Archaeometry Laboratory is supported by the National Science Foundation grant #2208558. Open access publication was facilitated by Università degli Studi di Napoli Federico II, as part of the Wiley - CRUI-CARE agreement.

DATA AVAILABILITY STATEMENT

The data that support the findings of this study are available from the corresponding author upon reasonable request.

ORCID

Maria Verde  <http://orcid.org/0000-0002-1661-2613>
 Alberto De Bonis  <http://orcid.org/0000-0002-8088-9481>
 Massimo D'Antonio  <https://orcid.org/0000-0003-2077-943X>
 Virginie Renson  <http://orcid.org/0000-0002-5701-0985>
 Stephen Czujko  <https://orcid.org/0009-0003-6617-4265>
 Vincenzo Morra  <https://orcid.org/0000-0002-3310-8603>

REFERENCES

Arienzo, I., Carandente, A., Di Renzo, V., Belviso, P., Civetta, L., D'Antonio, M., & Orsi, G. (2013). Sr and Nd isotope analysis at the Radiogenic Isotope Laboratory of the Istituto Nazionale di Geofisica e Vulcanologia, Sezione di Napoli—Osservatorio Vesuviano. *Rapporti Tecnici INGV*, 260, 1–18.

Arnold, D. (2006). The threshold model for ceramic resources: A refinement. In D. Gheorghiu (Ed.), *Ceramic studies: Papers on social and cultural significance of ceramics in Europe and Eurasia from prehistoric to historic times* (1553, pp. 3–9). British Archaeological Reports International Series.

De Astis, G., Pappalardo, L., & Piochi, M. (2004). Procida volcanic history: new insights into the evolution of the Phlegraean Volcanic District (Campania region, Italy). *Bulletin of Volcanology*, 66, 622–641.

Bonardi, G., Ciarcia, S., Di Nocera, S., Matano, F., Sgrossi, I., & Torre, M. (2009). Carta delle principali Unità Cinematiche dell'Appennino meridionale. *Bollettino della Società Geologica Italiana*, 128.

De Bonis, A., Arienzo, I., D'Antonio, M., Franciosi, L., Germinario, C., Grifa, C., Guarino, V., Langella, A., & Morra, V. (2018). Sr-Nd isotopic fingerprinting as a tool for ceramic provenance: Its application on raw materials, ceramic replicas and ancient pottery. *Journal of Archaeological Science*, 94, 51–59.

De Bonis, A., Cultrone, G., Grifa, C., Langella, A., & Morra, V. (2014). Clays from the Bay of Naples (Italy): New insight on ancient and traditional ceramics. *Journal of the European Ceramic Society*, 34, 3229–3244.

De Bonis, A., Grifa, C., Cultrone, G., De Vita, P., Langella, A., & Morra, V. (2013). Raw materials for archaeological pottery from the campania region of Italy: A petrophysical characterization. *Geoarchaeology*, 28(5), 478–503.

Brown, R. J., Civetta, L., Arienzo, I., D'Antonio, M., Moretti, R., Orsi, G., Tomlinson, E. L., Albert, P. G., & Menzies, M. A. (2014). Geochemical and isotopic insights into the assembly, evolution and disruption of a magmatic plumbing system before and after a cataclysmic caldera-collapse eruption at Ischia volcano (Italy). *Contributions to Mineralogy and Petrology*, 168, 1035.

Carter, S. R., Evensen, N. M., Hamilton, P. J., & O'Nions, R. K. (1978). Continental volcanics derived from enriched and depleted source regions: Nd-and Sr-isotope evidence. *Earth and Planetary Science Letters*, 37(3), 401–408.

Carter, S. W., Wiegand, B., Mahood, G. A., Dudas, F. O., Wooden, J. L., Sullivan, A. P., & Bowring, S. A. (2011). Strontium isotopic evidence for prehistoric transport of grayware ceramic materials in the eastern Grand Canyon region, USA. *Geoarchaeology*, 26, 189–218.

Conticelli, S., D'Antonio, M., Pinarelli, L., & Civetta, L. (2002). Source contamination and mantle heterogeneity in the genesis of Italian potassic and ultrapotassic volcanic rocks: Sr-Nd-Pb isotope data from Roman Province and Southern Tuscany. *Mineralogy and Petrology*, 74, 189–222.

Conticelli, S., Marchionni, S., Rosa, D., Giordano, G., Boari, E., & Avanzinelli, R. (2009). Shoshonite and sub-alkaline magmas from an ultrapotassic volcano: Sr-Nd-Pb isotope data on the Roccamontefina volcanic rocks, Roman Magmatic Province, southern Italy. *Contributions to Mineralogy and Petrology*, 157, 41–63.

D'Antonio, M., Mariconte, R., Arienzo, I., Mazzeo, F. C., Carandente, A., Perugini, D., Petrelli, M., Corselli, C., Orsi, G., Principato, M. S., & Civetta, L. (2016). Combined Sr-Nd isotopic and geochemical fingerprinting as a tool for identifying tephra layers: Application to deep-sea cores from Eastern Mediterranean Sea. *Chemical Geology*, 443, 121–136.

D'Antonio, M., Tilton, G. R., & Civetta, L. (1996). Petrogenesis of Italian alkaline lavas deduced from Pb-Sr-Nd isotope relationships. In A. Basu, & S. R. Hart (Eds.), *Earth processes: Reading the isotopic code: Geophysical Monograph Series* (Vol. 95, pp. 253–267). AGU.

D'Antonio, M., Tonarini, S., Arienzo, I., Civetta, L., Dallai, L., Moretti, R., Orsi, G., Andria, M., & Trecalli, A. (2013). Mantle and crustal processes in the magmatism of the Campania region: Inferences from mineralogy, geochemistry, and Sr-Nd-O isotopes of young hybrid volcanics of the Ischia Island (South Italy). *Contributions to Mineralogy and Petrology*, 165, 1173–1194.

D'Antonio, M., Tonarini, S., Arienzo, I., Civetta, L., & Di Renzo, V. (2007). Components and processes in the magma genesis of the Phleorean Volcanic District, southern Italy. In L. Beccaluva, G. Bianchini & M. Wilson (Eds.), *Cenozoic volcanism in the Mediterranean area*. (Geological Society of America Special Papers 418) (pp. 203–220). Geological Society of America.

Deines, P., Goldstein, S. L., Oelkers, E. H., Rudnick, R. L., & Walter, L. M. (2003). Standards for publication of isotope ratio and chemical data in chemical geology. *Chemical Geology*, 202, 1–4.

Fabbri, B., Gualtieri, S., & Shoval, S. (2014). The presence of calcite in archeological ceramics. *Journal of the European Ceramic Society*, 34, 1899–1911.

Faure, G., & Mensing, T. M. (2005). *Isotopes: Principles and applications*. John Wiley & Sons.

Galer, S. J. G. (1998). Practical application of lead triple spiking for correction of instrumental mass discrimination. *Mineralogical Magazine*, 62A, 491–492.

Galli, P., Giaccio, B., Messina, P., Peronace, E., Amato, V., Naso, G., Nomade, S., Pereira, A., Piscitelli, S., Bellanova, J., Billi, A., Blamart, D., Galderisi, A., Giocoli, A., Stabile, T., & Thil, F. (2017). Middle to Late Pleistocene activity of the northern Matese fault system (southern Apennines, Italy). *Tectonophysics*, 699, 61–81.

Giaccio, B., Hajdas, I., Isaia, R., Deino, A., & Nomade, S. (2017). High-precision ^{14}C and $^{40}\text{Ar}/^{39}\text{Ar}$ dating of the Campanian Ignimbrite (Y-5) reconciles the time-scales of climatic-cultural processes at 40 ka. *Scientific Reports*, 7(1), 45940.

Guarino, V., De Bonis, A., Grifa, C., Langella, A., Morra, V., & Pedroni, L. (2011). Archaeometric study on terra sigillata from Cales (Italy). *Periodico di Mineralogia*, 80, 455–470.

Guarino, V., De Bonis, A., Peña, J. T., Verde, M., & Morra, V. (2021). Multianalytical investigation of wasters from the Tower 8/Porta di Nola refuse middens in Pompeii: Sr–Nd isotopic, chemical, petrographic, and mineralogical analyses. *Geoarchaeology*, 36, 712–739.

Hawkesworth, C. J., & Vollmer, R. (1979). Crustal contamination versus enriched mantle: $143\text{Nd}/144\text{Nd}$ and $87\text{Sr}/86\text{Sr}$ evidence from the Italian volcanics. *Contributions to Mineralogy and Petrology*, 69, 151–165.

Kibaroglu, M., Kozal, E., Klügel, A., Hartmann, G., & Monien, P. (2019). New evidence on the provenance of Red Lustrous Wheel-made Ware (RLW): Petrographic, elemental and Sr–Nd isotope analysis. *Journal of Archaeological Science: Reports*, 24, 412–433.

Langmuir, C. H., Vocke, Jr. R. D., Hanson, G. N., & Hart, S. R. (1978). A general mixing equation with applications to Icelandic basalts. *Earth and Planetary Science Letters*, 37(1), 380–392.

Li, B. P., Zhao, J. X., Greig, A., Collerson, K. D., Feng, Y. X., Sun, X. M., Guo, M. S., & Zhuo, Z. X. (2006). Characterisation of Chinese Tang sancai from Gongxian and Yaozhou kilns using ICP-MS trace element and TIMS Sr–Nd isotopic analysis. *Journal of Archaeological Science*, 33, 56–62.

Li, B. P., Zhao, J. X., Greig, A., Collerson, K. D., Zhuo, Z. X., & Feng, Y. X. (2005). Potential of Sr isotopic analysis in ceramic provenance studies: Characterisation of Chinese stonewares. *Nuclear Instruments and Methods in Physics Research*, B, 240, 726–732.

Maggetti, M. (2001). Chemical analyses of ancient ceramics: What for CHIMIA. *International Journal of Chemistry*, 55, 923–930.

Makarona, C., Mattielli, N., Laha, P., Terryn, H., Nys, K., & Claeys, P. (2016). Leave no mudstone unturned: Geochemical proxies for provenancing mudstone temper sources in South-Western Cyprus. *Journal of Archaeological Science: Reports*, 7, 458–464.

Maritan, L., Gravagna, E., Cavazzini, G., Zerboni, A., Mazzoli, C., Grifa, C., Mercurio, M., Mohamed, A. A., Usai, D., & Salvatori, S. (2023). Nile River clayey materials in Sudan: Chemical and isotope analysis as reference data for ancient pottery provenance studies. *Quaternary International*, 657, 50–66.

Orsi, G., D'Antonio, M., & Civetta, L. (2022). Introduction. In G. Orsi, M. D'Antonio, & L. Civetta (Eds.), *Campi Flegrei. Active volcanoes of the world* (pp. vii–x). Springer.

Pabst, S., Wörner, G., Civetta, L., & Tesoro, R. (2008). Magma chamber evolution prior to the Campanian ignimbrite and Neapolitan Yellow Tuff eruptions (Campi Flegrei, Italy). *Bulletin of Volcanology*, 70, 961–976.

Paone, A. (2006). The geochemical evolution of the Mt. Somma-Vesuvius volcano. *Mineralogy and Petrology*, 87, 53–80.

Pappalardo, L., Piochi, M., D'Antonio, M., Civetta, L., & Petrini, R. (2002). Evidence for multi stage magmatic evolution during the past 60 kyr at Campi Flegrei (Italy) deduced from Sr, Nd and Pb isotope data. *Journal of Petrology*, 43(8), 1415–1434.

Pedroni, L. (2001). *Ceramica calena a vernice nera. Produzione e diffusione*. Petrucci Editore.

Plank, T., & Langmuir, C. H. (1998). The chemical composition of subducting sediment and its consequences for the crust and mantle. *Chemical Geology*, 145(3–4), 325–394.

Renson, V., Coenaerts, J., Nys, K., Mattielli, N., Vanhaecke, F., Fagel, N., & Claeys, P. (2011). Lead isotopic analysis for the identification of Late Bronze Age pottery from hala sultan tekke (Cyprus): Lead isotopic analysis of Late Bronze Age pottery from Hala Sultan Tekke. *Archaeometry*, 53(1), 37–57.

Renson, V., Jacobs, A., Coenaerts, J., Mattielli, N., Nys, K., & Claeys, P. (2013). Using lead isotopes to determine pottery provenance in Cyprus: Clay source signatures and comparison with Late Bronze Age Cypriote pottery. *Geoarchaeology*, 28(6), 517–530.

Renson, V., Martínez-Cortizas, A., Mattielli, N., Coenaerts, J., Sauvage, C., De Vleeschouwer, F., Lorre, C., Vanhaecke, F., Bindler, R., Rautman, M., Nys, K., & Claeys, P. (2013). Lead isotopic analysis within a multi-proxi approach to trace pottery sources. The example of White Slip II sherds from Late Bronze Age sites in Cyprus and Syria. *Applied Geochemistry*, 28, 220–234.

Renson, V., Slane, K. W., Rautman, M. L., Kidd, B., Guthrie, J., & Glascock, M. D. (2016). Pottery provenance in the eastern Mediterranean using lead isotopes. *Archaeometry*, 58, 54–67.

Di Renzo, V., Arienzo, I., Civetta, L., D'Antonio, M., Tonarini, S., Di Vito, M. A., & Orsi, G. (2011). The magmatic feeding system of the Campi Flegrei caldera: Architecture and temporal evolution. *Chemical Geology*, 281, 227–241.

Di Renzo, V., Di Vito, M. A., Arienzo, I., Carandente, A., Civetta, L., D'Antonio, M., Giordano, F., Orsi, G., & Tonarini, S. (2007). Magmatic history of Somma-Vesuvius on the basis of new geochemical and isotopic data from a deep borehole (Camaldoli della Torre). *Journal of Petrology*, 48, 753–784.

De Rita, D., & Giordano, G. (1996). Volcanological and structural evolution of Roccamontefina volcano (southern Italy). In W. J. McGuire, A. P. Jones, & J. Neuberg (Eds.), *Volcano instability on the earth and other planets* (Vol. 110, pp. 209–224). Geological Society.

Rollinson, H., & Pease, V. (2021). *Using geochemical data: To understand geological processes*. University Printing House, Cambridge CB2 8BS.

Soricelli, G. (2004). La produzione di terra sigillata in Campania, in Early Italian Sigillata. In J. Poblome, P. Talloen, R. Brulet, & M. Waelkens (Eds.), *The Chronological framework and trade patterns* (pp. 299–307). Peeters Publishers.

Tonarini, S., D'Antonio, M., Di Vito, M. A., Orsi, G., & Carandente, A. (2009). Geochemical and B–Sr–Nd isotopic evidence for mingling and mixing processes in the magmatic system that fed the Astroni volcano (4.1–3.8 ka) within the Campi Flegrei caldera (Southern Italy). *Lithos*, 107(3–4), 135–151.

Verde, M., De Bonis, A., Renson, V., Germinario, C., Rispoli, C., D'Uva, F., Tomeo, A., & Morra, V. (2023). Minero-petrographic characterization of fine ware from Cales (South Italy). *Archaeometry*, 65(6), 1145–1184.

Vitale, S., & Ciarcia, S. (2018). Tectono-stratigraphic setting of the Campania region (Southern Italy). *Journal of Maps*, 14, 9–21.

Weis, D., Kieffer, B., Maerschalk, C., Barling, J., De Jong, J., Williams, G. A., Hanano, D., Pretorius, W., Mattielli, N., Scoates, J. S., Goolaerts, A., Friedman, R. M., & Mahoney, J. B. (2006). High-precision isotopic characterization of USGS reference materials by TIMS and MC-ICP-MS. *Geochemistry, Geophysics, Geosystems*, 7(8), 1–30.

White, W. M., Albarède, F., & Télouk, P. (2000). High-precision analysis of Pb isotope ratios by multi-collector ICP-MS. *Chemical Geology*, 167, 257–270.

Zhang, W., & Hu, Z. (2020). Estimation of isotopic reference values for pure materials and geological reference materials. *Atomic Spectroscopy*, 41, 93–102.

SUPPORTING INFORMATION

Additional supporting information can be found online in the Supporting Information section at the end of this article.

How to cite this article: Verde, M., De Bonis, A., D'Antonio, M., Renson, V., Czujko, S., Tomeo, A., & Morra, V. (2024). Unveiling the distinctive geochemical signature of fine ware through Sr–Nd–Pb isotopes: A site-specific perspective from the site of Cales (South Italy). *Geoarchaeology*, 1–15.

<https://doi.org/10.1002/gea.22021>